

Copper(i) dye-sensitized solar cells with  $[\text{Co}(\text{bpy})_3]^{2+/3+}$  electrolyte†Cite this: *Chem. Commun.*, 2013, **49**, 7222Received 19th June 2013,  
Accepted 4th July 2013

DOI: 10.1039/c3cc44595j

www.rsc.org/chemcomm

**The hierarchical assembly of DSCs containing a new heteroleptic copper(i) complex with a phosphonic acid anchoring ligand is described; it is shown that conventional  $\Gamma^-/\text{I}_3^-$  electrolytes may be replaced by  $[\text{Co}(\text{bpy})_3]^{2+/3+}$  with no loss in performance.**

Dye-sensitized solar cells (DSCs) are photovoltaic devices in which the response of a semiconductor is extended into the visible region by use of a coloured sensitizer.<sup>1</sup> Attention is centred upon the replacement of first generation sensitizers based on ruthenium complexes by those using other metals or organic dyes. Copper(i) complexes  $[\text{Cu}(\text{L}_{\text{anc}})(\text{L})]^{+}$  are leading contenders for use as dyes based on Earth abundant metals.<sup>2</sup> We are currently optimizing the performance of DSCs based on copper(i) complexes and report in this paper on (i) the improvement of the spectral response of the dyes (ii) the stability of the surface-bound dyes and (iii) the long-term stability of the DSC.

We have developed procedures for the assembly of heteroleptic copper(i) dyes by ligand exchange between a surface-anchored ligand  $\text{L}_{\text{anc}}$  and  $[\text{Cu}(\text{L})_2]^{+}$ .<sup>3–7</sup> Pellegrin, Daniel, Odobel and coworkers<sup>8</sup> have reported DSCs with an extended spectral response utilizing a 2-(diarylamino-phenyl)-1*H*-phenanthro[9,10-*d*]imidazole ancillary ligand.<sup>8</sup> We now describe our studies of DSCs using related ligands, which both give improved spectral characteristics and improve the stability of the heteroleptic complexes (phen complexes are typically one log *K* unit more stable than bpy analogues). Optimal performance is achieved with phosphonic acid anchors, which both stabilize the surface-bound complex with respect to carboxylate  $\text{L}_{\text{anc}}$  systems and lead to enhanced energy conversion efficiencies.<sup>4–7,9</sup> The inclusion of an aryl spacer between bpy-unit and  $\text{PO}(\text{OH})_2$ -anchor is beneficial.<sup>7</sup> Finally, the long term stability of the DSC (which may be limited by the formation of CuI in the presence of  $\Gamma^-/\text{I}_3^-$  electrolyte) has been addressed by changing to a  $[\text{Co}(\text{bpy})_3]^{2+}/[\text{Co}(\text{bpy})_3]^{3+}$  electrolyte.<sup>10</sup> This latter change has been coupled with modifications of the photoanode at the

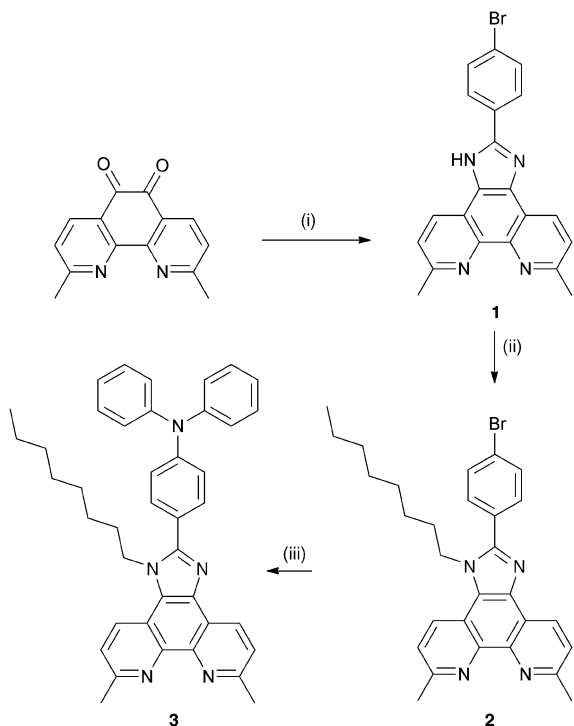
mesoscopic level, specifically by changing the semiconductor film thickness<sup>11,12</sup> and by post-treatment with  $\text{H}_2\text{O}-\text{TiCl}_4$ .<sup>13</sup>

The ancillary ligand L facilitates light-harvesting and 2-(4-bromophenyl)-1*H*-phenanthro[9,10-*d*]imidazole<sup>14</sup> provides a convenient starting point for the design of a ligand family. The first design feature is the introduction of 6,6'-dialkyl or diaryl substituents to stabilize the copper(i) oxidation state.<sup>15</sup> The second is the incorporation of a triphenylamino-substituent to extend the  $\pi$ -conjugation and increase the spectral response. The third is the introduction of a long chain substituent which is known to suppress intermolecular aggregation by preventing extensive face-to-face  $\pi$ -interactions between aromatic units.<sup>16</sup> Self-assembly of dyes at the semiconductor surface produces a hydrophobic monolayer that repels iodide ions in the  $\Gamma^-/\text{I}_3^-$  electrolyte thereby reducing the rate of recombination and increasing the open circuit voltage ( $V_{\text{oc}}$ ).<sup>17</sup>

Scheme 1 summarizes our synthetic approach to a first generation ligand starting from 2,9-dimethyl-1,10-phenanthroline-5,6-dione.<sup>18</sup> Treatment of the latter with 4-bromobenzaldehyde and an excess of  $\text{NH}_4\text{OAc}$  in ethanol yielded compound **1**. The <sup>1</sup>H and <sup>13</sup>C NMR spectra are consistent with a tautomeric equilibrium involving the imidazole NH and N sites.† *In situ* deprotonation of **1** and reaction with *n*-octyl bromide yielded **2** which was fully characterized.† The highest mass peak in the electrospray mass spectrum (*m/z* 515.2) corresponded to the  $[\text{M} + \text{H}]^+$  ion. In contrast to **1**, the NMR spectra are desymmetrized and two signals are observed ( $\delta$  2.98 and 2.96 ppm in  $\text{CDCl}_3$ ) for the  $\text{H}^{\text{Me-phen}}$  protons. Single crystals were grown from a toluene-ethyl acetate solution, and Fig. 1 shows the structure of **2**.† The octyl chain is ordered and lies over the bromophenyl unit, the arene ring of which is twisted 58.6° out of the plane of the imidazole ring. The conformation of the octyl chain allows close  $\text{CH}\cdots\pi$  and  $\text{CH}\cdots\text{Br}$  contacts; the distance  $\text{C}29\text{H}29\text{A}\cdots\text{Br}1$  of 3.12 Å is close to the sum of the van der Waals radii, using a value of 1.10 Å<sup>19</sup> for H rather than the Bondi value of 1.20 Å.<sup>20</sup> The closest  $\text{CH}\cdots\pi$  contacts are 3.30 and 3.66 Å. Buchwald-Hartwig amination of **2** with diphenylamine resulted in the formation of **3**; the highest mass peak in the ESI MS (*m/z* 604.3) arises from  $[\text{M} + \text{H}]^+$ , and the <sup>1</sup>H and <sup>13</sup>C NMR spectra are consistent with the structure shown in Scheme 1.

Department of Chemistry, University of Basel, Spitalstrasse 51, CH4056 Basel, Switzerland. E-mail: edwin.constable@unibas.ch, catherine.housecroft@unibas.ch; Tel: +41 61 267 1008

† Electronic supplementary information (ESI) available: Experimental data. Fig. S1: EQE spectra. CCDC 945455. For ESI and crystallographic data in CIF or other electronic format see DOI: 10.1039/c3cc44595j



**Scheme 1** Synthesis of ligand **3**. Conditions: (i) 4-bromobenzaldehyde, excess  $\text{NH}_4\text{OAc}$ , EtOH, 91%; (ii) NaH, DMF, *n*-octyl bromide, 75 °C, 15 h; (iii)  $\text{Ph}_2\text{NH}$ ,  $\text{Pd}(\text{bda})_2/\text{P}^t\text{Bu}_3$ , toluene, reflux overnight, 52%.†

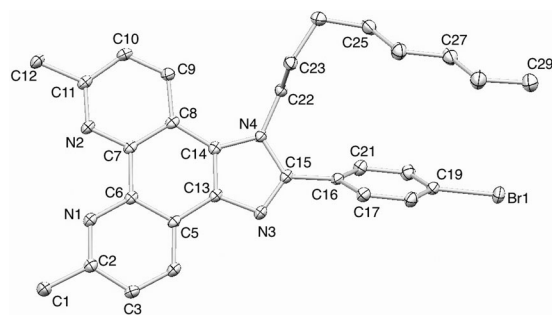


**Fig. 1** Structure of compound **2** (ellipsoids plotted at 40% probability level and H atoms omitted for clarity).

The homoleptic complex  $[\text{Cu}(\mathbf{3})_2][\text{PF}_6]$  was prepared in quantitative yield by reaction of  $[\text{Cu}(\text{NCMe})_4][\text{PF}_6]$  with two equivalents of **3**. The MALDI mass spectrum showed peaks at  $m/z$  1271.6 and 666.9 corresponding to  $[\text{M} - \text{PF}_6]^+$  and  $[\text{M} - 3\text{-PF}_6]^+$  with isotope patterns matching those calculated. The  $^1\text{H}$  and  $^{13}\text{C}$  NMR spectra were consistent with a single ligand environment, the presence of the octyl chain desymmetrizing the phenanthro[9,10-*d*]imidazole unit.† Fig. 2 compares the solution absorption spectra of **3** and  $[\text{Cu}(\mathbf{3})_2][\text{PF}_6]$ . The approximate doubling of the extinction coefficients of the bands (assigned to  $\pi^* \leftarrow \pi$  and  $\pi^* \leftarrow n$  transitions) in the UV region is consistent with the presence of two ligands in the complex. The spectral response of the complex extends to 600 nm, with  $\lambda_{\text{max}}$  for the MLCT band at 476 nm. Reversible oxidation of the Cu(I) centre in  $[\text{Cu}(\mathbf{3})_2][\text{PF}_6]$  occurs at +0.42 V, compared to +0.50 V (vs.  $\text{Fc}/\text{Fc}^+$  in  $\text{CH}_2\text{Cl}_2$ ) for  $[\text{Cu}(\text{dmp})_2][\text{PF}_6]$  ( $\text{dmp}$  = 2,9-dimethyl-1,10-phenanthroline).<sup>21</sup> A second oxidation process at +0.63 V is most

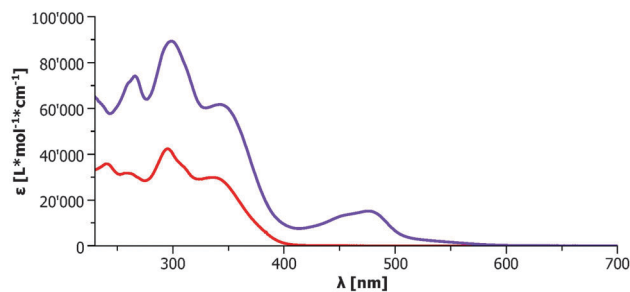
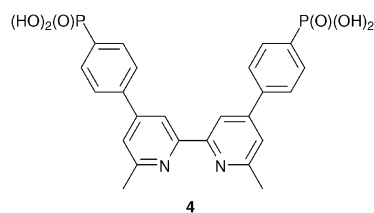


**Fig. 2** Absorption spectra of **3** (red) and  $[\text{Cu}(\mathbf{3})_2][\text{PF}_6]$  (blue) in  $\text{CH}_2\text{Cl}_2$ .



**Scheme 2** Structure of anchoring ligand **4**.

probably associated with oxidation of the  $\text{Ph}_2\text{N}$  unit. No reduction processes are observed within the solvent accessible window.

Fully masked DSCs<sup>22</sup> were fabricated by applying a scattering  $\text{TiO}_2$  layer to screen-printed mesoporous  $\text{TiO}_2$  (3 or 4 layers) followed by post-treatment with  $\text{H}_2\text{O}-\text{TiCl}_4$ ,<sup>13</sup> and then soaking the cells in a solution of anchoring ligand **4** (Scheme 2). This was followed by a period of 24, 64 or 110 hours soaking in solutions of  $[\text{Cu}(\mathbf{3})_2][\text{PF}_6]$ . During this period, the surface-anchored heteroleptic complex  $[\text{Cu}(\mathbf{3})(\mathbf{4})]^+$  was formed (see experimental details).† We first assessed the DSC characteristics of cells containing  $\Gamma^-/\text{I}_3^-$  electrolyte and  $[\text{Cu}(\mathbf{3})(\mathbf{4})]^+$  sensitizer supported on 3 layers of  $\text{TiO}_2$  post-treated with different concentrations of  $\text{H}_2\text{O}-\text{TiCl}_4$ . Table 1 summarizes measurements made on the day of sealing the cells. *I-V* characteristics of the same cells were recorded one, six and eight days after sealing, and only small changes in values of  $J_{\text{SC}}$ ,  $V_{\text{OC}}$  and  $\eta$  were observed, in contrast to the ripening effects noted with other copper-based DSCs.<sup>4,6,7</sup> Post-treatment with 5  $\text{mmol dm}^{-3}$   $\text{H}_2\text{O}-\text{TiCl}_4$  results in improved  $J_{\text{SC}}$  and  $V_{\text{OC}}$  values with concomitant increase in efficiency. Treatment of 3 layers of  $\text{TiO}_2$  post-treated with higher concentrations had little or no effect on the overall energy conversion efficiencies of the DSCs. The effect of replacing  $\Gamma^-/\text{I}_3^-$  electrolyte by  $[\text{Co}(\text{bpy})_3]^{2+}/[\text{Co}(\text{bpy})_3]^{3+}$  is seen by comparing the data in Tables 1 and 2. For all the cells in Table 1 and the top half of Table 2, the photoanodes were left to stand in solutions of  $[\text{Cu}(\mathbf{3})_2][\text{PF}_6]$  for 24 hours. The results suggest that energy conversion efficiency is increased by using higher concentrations of  $\text{TiCl}_4$  during post-treatment. Since dye

**Table 1** DSC performances using  $[\text{Cu}(\mathbf{3})_2][\text{PF}_6]$ , anchor **4**,  $\Gamma^-/\text{I}_3^-$  electrolyte, and 3 layers of  $\text{TiO}_2$ ; dipping time = 24 h. Measurements made on the day of sealing

$[\text{TiCl}_4]/\text{mmol dm}^{-3}$	$J_{\text{SC}}/\text{mA cm}^{-2}$	$V_{\text{OC}}/\text{mV}$	ff	$\eta/\%$
0	1.99	588	0.69	0.80
5	2.73	612	0.70	1.18
15	2.00	608	0.67	0.81
30	2.25	599	0.65	0.88
40	2.11	591	0.64	0.80
60	2.34	592	0.64	0.89

**Table 2** DSC performances using  $[\text{Cu}(\text{3})_2]^+$ , anchor **4**,  $[\text{Co}(\text{bpy})_3]^{2+/3+}$  and 3 layers  $\text{TiO}_2$ . Measurements were made on day of sealing the cell

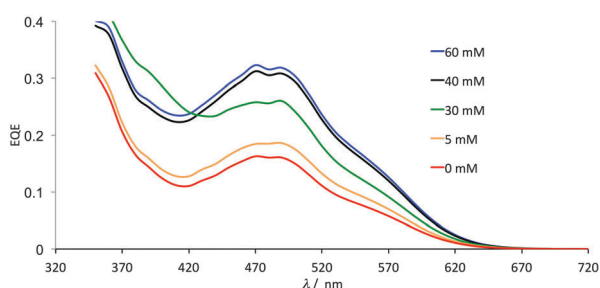
$[\text{TiCl}_4]/\text{mmol dm}^{-3}$	$J_{\text{SC}}/\text{mA cm}^{-2}$	$V_{\text{OC}}/\text{mV}$	ff	$\eta/\%$
Cells dipped into solution of $[\text{Cu}(\text{3})_2][\text{PF}_6]$ for 24 h				
0	1.15	380	0.49	0.22
5	1.75	535	0.53	0.50
15	1.62	564	0.56	0.51
30	1.56	590	0.61	0.56
40	2.20	542	0.55	0.66
60	3.17	596	0.63	1.19
Cells dipped into solution of $[\text{Cu}(\text{3})_2][\text{PF}_6]$ for 64 h				
0	2.28	586	0.55	0.73
5	1.83	611	0.62	0.69
15	3.44	628	0.70	1.50
30	3.48	619	0.70	1.51
40	2.87	621	0.68	1.21
60	2.28	586	0.55	0.73

**Table 3** DSC performances with  $[\text{Cu}(\text{3})_2]^+$ , anchor **4**,  $[\text{Co}(\text{bpy})_3]^{2+/3+}$  and 4 layers  $\text{TiO}_2$ ; dipping time 110 h. Measurements made on day of sealing

$[\text{TiCl}_4]/\text{mmol dm}^{-3}$	$J_{\text{SC}}/\text{mA cm}^{-2}$	$V_{\text{OC}}/\text{mV}$	ff	$\eta/\%$
0	3.01	545	0.51	0.83
5	3.33	505	0.51	0.85
15	2.39	391	0.51	0.48
30	3.39	427	0.52	0.75
40	5.05	578	0.59	1.73
60	4.95	610	0.67	2.02

uptake by the  $\text{TiO}_2$  is affected by the time over which the photoanodes are left to soak in solutions of the dye, we prepared a set of DSCs with a dipping time of 64 hours. In all other respects, the DSC fabrication was the same as that of cells in which the dipping time was 24 hours. Cell characteristics (Table 2) show that a longer soaking time leads to superior performance, and that the optimum concentrations of  $\text{H}_2\text{O}-\text{TiCl}_4$  during post-treatment are  $>15 \text{ mmol dm}^{-3}$ . The external quantum efficiency (EQE) spectra for four of the DSCs in the top part of Table 2 are shown in Fig. S1 (ESI<sup>†</sup>), and confirm that the highest concentration of  $\text{TiCl}_4$  leads to the highest EQE ( $\approx 20\%$ ) and improved photon-to-current conversion efficiencies, especially at longer wavelengths.

Comparison of the data in Tables 2 and 3 reveals a significant improvement of cell performance upon increasing the thickness of screen-printed  $\text{TiO}_2$  from 3 to 4 layers. A longer dipping time (110 hours) was used, and a maximum efficiency ( $\eta$ ) of 2.02% was achieved with a post-treatment of  $60 \text{ mmol dm}^{-3} \text{ H}_2\text{O}-\text{TiCl}_4$ . Trends in data are generally maintained for measurements made with duplicate cells and give maximum values of  $\eta$  with 40 or  $60 \text{ mmol dm}^{-3}$

**Fig. 3** EQE spectra for five of the DSCs listed in Table 3.

$\text{H}_2\text{O}-\text{TiCl}_4$ , but absolute values of  $\eta$  show variation. Fig. 3 shows corresponding EQE spectra; a maximum photon-to-current conversion efficiency of 32% is observed. For comparison, 4-layer DSCs were made using  $\Gamma/\text{I}_3^-$  electrolyte retaining  $[\text{Cu}(\text{3})(\text{4})]^+$  as dye and a dipping time of 110 h. With post-treatment of  $40 \text{ mmol dm}^{-3} \text{ H}_2\text{O}-\text{TiCl}_4$ , the cell characteristics were  $J_{\text{SC}} = 5.11 \text{ mA cm}^{-2}$ ,  $V_{\text{OC}} = 574 \text{ mV}$ ,  $\text{ff} = 0.71$  and  $\eta = 2.08\%$  (compared to  $\eta = 6.90\%$  for an analogous DSC using N719). Preliminary light-stability tests in which post-treated 4-layer DSCs containing anchored- $[\text{Cu}(\text{3})(\text{4})]^+$  dye and  $[\text{Co}(\text{bpy})_3]^{2+/3+}$  or  $\Gamma/\text{I}_3^-$  electrolyte were continuously illuminated ( $100 \text{ mW cm}^{-2}$ ) indicate that all cells show similar stabilities over a 60 hour period.

After optimization, the efficiencies of DSCs containing  $[\text{Cu}(\text{3})(\text{4})]^+$  dye anchored on  $\text{H}_2\text{O}-\text{TiCl}_4$  post-treated 4 layer  $\text{TiO}_2$  are comparable using either  $[\text{Co}(\text{bpy})_3]^{2+/3+}$  or  $\Gamma/\text{I}_3^-$  electrolyte. This is the first report of DSCs which combine copper(i)-based dyes and  $[\text{Co}(\text{bpy})_3]^{2+/3+}$  electrolyte, and is a critical step towards the development of stable iodide-free copper(i) solar cells.

The European Research Council (Advanced Grant 267816 LiLo), Swiss National Science Foundation and University of Basel are acknowledged for financial support. Nik Hostettler and Dr Colin Martin recorded 500 MHz NMR spectra, and Gino Günzburger and Ewald Schönhofer assisted with DSC stability tests.

## Notes and references

- 1 K. Kalyanasundaram, *Dye-sensitized Solar Cells*, EPFL Press, Lausanne, 2010.
- 2 B. Bozic-Weber, E. C. Constable and C. E. Housecroft, *Coord. Chem. Rev.*, 2013, DOI: 10.1016/j.ccr.2013.05.019.
- 3 A. H. Redondo, E. C. Constable and C. E. Housecroft, *Chimia*, 2009, **63**, 205.
- 4 B. Bozic-Weber, V. Chaurin, E. C. Constable, C. E. Housecroft, M. Meuwly, M. Neuberger, J. A. Rudd, E. Schönhofer and L. Siegfried, *Dalton Trans.*, 2012, **41**, 14157.
- 5 B. Bozic-Weber, E. C. Constable, C. E. Housecroft, P. Kopecky, M. Neuberger and J. A. Zampese, *Dalton Trans.*, 2011, **40**, 12584.
- 6 B. Bozic-Weber, S. Y. Brauchli, E. C. Constable, S. O. Furer, C. E. Housecroft and I. A. Wright, *Phys. Chem. Chem. Phys.*, 2013, **15**, 4500.
- 7 B. Bozic-Weber, S. Y. Brauchli, E. C. Constable, S. O. Furer, C. E. Housecroft, F. J. Malzner, I. A. Wright and J. A. Zampese, *Dalton Trans.*, 2013, DOI: 10.1039/c3dt51416a.
- 8 M. Sandroni, M. Kayanuma, A. Planchat, N. Szuwarski, E. Blart, Y. Pellegrin, C. Daniel, M. Boujtita and F. Odobel, *Dalton Trans.*, 2013, DOI: 10.1039/c3dt50852h.
- 9 P. Péchy, F. P. Rotzinger, Md. K. Nazeeruddin, O. Kohle, S. M. Zakeeruddin, R. Humphry-Baker and M. Grätzel, *J. Chem. Soc., Chem. Commun.*, 1995, 65.
- 10 T. W. Hamann, *Dalton Trans.*, 2012, **41**, 3111.
- 11 S. M. Feldt, E. A. Gibson, E. Gabrielsen, L. Sun, G. Boschloo and A. Hagfeldt, *J. Am. Chem. Soc.*, 2010, **132**, 16714.
- 12 E. A. Gibson, A. L. Smeigh, L. Le Pleux, L. Hammarström, F. Odobel, G. Boschloo and A. Hagfeldt, *J. Phys. Chem. C*, 2011, **115**, 9772.
- 13 S.-W. Lee, K.-S. Ahn, K. Zhu, N. R. Neale and A. J. Frank, *J. Phys. Chem.*, 2012, **116**, 21285; P. M. Sommeling, B. C. O'Regan, R. R. Haswell, H. J. P. Smit, N. J. Bakker, J. J. T. Smits, J. M. Kroon and J. A. M. van Roosmalen, *J. Phys. Chem. B*, 2006, **110**, 19191; B. C. O'Regan, J. R. Durrant, P. M. Sommeling and N. J. Bakker, *J. Phys. Chem. C*, 2007, **111**, 14001.
- 14 D. W. Allen, J. Hawkrigg, H. Adams, B. F. Taylor, D. E. Hibbs and M. B. Hursthouse, *J. Chem. Soc., Perkin Trans. 1*, 1998, 335.
- 15 W. B. Brandt, F. P. Dwyer and E. D. Gyrfas, *Chem. Rev.*, 1954, **545**, 959.
- 16 Y. Ooyama and Y. Harima, *Eur. J. Org. Chem.*, 2009, 2903.
- 17 Md. K. Nazeeruddin, E. Baranoff and M. Grätzel, *Sol. Energy*, 2011, **85**, 1172.
- 18 R. H. Zheng, H. C. Guo, H. J. Jiang, K. H. Xu, B. B. Liu, W. L. Sun and Z. Q. Shen, *Chin. Chem. Lett.*, 2010, 1270.
- 19 R. S. Rowland and R. Taylor, *J. Phys. Chem.*, 1996, **100**, 7384.
- 20 A. Bondi, *J. Phys. Chem.*, 1964, **68**, 441.
- 21 M. K. Eggleston, D. R. McMillin, K. S. Koenig and A. J. Pallenberg, *Inorg. Chem.*, 1997, **36**, 172.
- 22 H. J. Snaith, *Energy Environ. Sci.*, 2012, **5**, 6513.